Optical Design of Dilute Nitride Quantum Wells Vertical Cavity Semiconductor Optical Amplifiers for Communication Systems

Faten A. Chaqmaqchee

Department of Physics, Faculty of Science and Health, Koya University
Daniel Mitterrand Boulevard, Koya KOY45, Kurdistan Region – F.R. Iraq

***Abstract*—III-V semiconductors components such as Gallium Arsenic (GaAs), Indium Antimony (InSb), Aluminum Arsenic (AlAs) and Indium Arsenic (InAs) have high carrier mobilities and direct energy gaps. This is making them indispensable for today's optoelectronic devices such as semiconductor lasers and optical amplifiers at 1.3 µm wavelength operation. In fact, these elements are led to the invention of the Gallium Indium Nitride Arsenic (GaInNAs), where the lattice is matched to GaAs for such applications. This article is aimed to design dilute nitride GaInNAs quantum wells (QWs) enclosed between top and bottom of Aluminum (Gallium) Arsenic Al(Ga)As distributed bragg mirrors (DBRs) using MATLAB® program. Vertical cavity semiconductor optical amplifiers (VCSOAs) structures are based on Fabry Perot (FP) method to design optical gain and bandwidth gain to be operated in reflection and transmission modes. The optical model gives access to the contact layer of epitaxial structure and the reflectivity for successive radiative modes, their lasing thresholds, emission wavelengths and optical field distributions in the laser cavity.**

***Index Terms*—Amplifier, Al(Ga)As, gain, GaInNAs, VCSOA.**

I. Introduction

Dilute nitride III-V alloys are essential for today's optoelectronic devices applications, such as lasers modulators, photodetectors and optical fibre communication systems. One potentially important material for such applications is the quaternary alloy GaInNAs (Kondow, et al. 1996; Buyanova, Chen and Monemar 2001). GaInNAs/GaAs quantum well (QW) based devices were originally proposed as replacements for GaInAs/InP QW based devices due to their reduced temperature sensitivity (Sun, et al., 2009). GaInNAs may be grown on GaAs, allowing the use of high quality Al(Ga)As/GaAs distributed Bragg reflectors (DBRs) for the long wavelength optical communications window. GaInNAs have potential cost advantages compared to indium phosphide (InP)-based approaches. It can be used to fabricate several devices, such as high performance laser diodes among which are vertical cavity surface emitting lasers (VCSELs) emitting in 1.3 µm window. The massive interest in VCSEL devices has focused on semiconductor optical amplifier (SOA) based VCSEL technology. Vertical cavity semiconductor optical amplifiers (VCSOAs) are important components in optical fiber networks. These devices have advantages over edge emitting lasers (EEL) and in plane- semiconductor optical amplifiers (SOAs) of various amplifier lengths. The vertical cavity geometry for such devices yields high coupling efficiency to optical fiber, which is useful for achieving a low noise figure with better performance. It also allows for single wavelength amplification, and two dimensional array fabrication; hence lowering the power consumption and manufacturing cost. The narrower bandwidth of the vertical cavity structures makes the devices also good for filtering applications (Piprek, Björlin and Bowers, 2001).

GaInNAs material has attracted attention by virtue of its unusual physical properties compared to conventional III-V compounds. By adding small amounts of nitrogen and Indium to GaAs, the whole wavelength range between 1.3 µm and 1.6 µm is reachable in principle. However as this material system has been explored the unique nature of the nitrogen (N) interaction with the GaInAs system has become apparent. This arises because the nitrogen is very electronegative and pushing the conduction band energy down as modeled successfully by the band anti-crossing (BAC) model (Shan, et al., 1999). When small amounts of nitrogen are introduced into (In)GaAs, a strong interaction occurs between the conduction band and a narrow resonant band formed by the highly localized nitrogen states E_N, as shown clearly in Fig.1 The nitrogen level is treated as a perturbation on the host material conduction band E_M; the effect of this is a splitting of the conduction band into two non-parabolic subbands, E_+ and E_-, The E_- is pushed downwards relative to E_M level, while the E_+ is pushed upwards relative to E_N level. The reduction in the energy of the E_- level is responsible for the observed decrease in emission energy (Skierbiszewski, et al., 2000).

ARO-The Scientific Journal of Koya University
Volume IV, No 1(2016), Article ID: ARO.10076, 05 pages
DOI: 10.14500/aro.10076
Received 29 March 2015; Accepted 02 March 2016
Regular research paper: Published 06 April 2016

Correspond. author's e-mail: faten.chaqmaqchee@koyauniversity.org
Copyright © 2016 Faten A. Chaqmaqchee. This is an open access article distributed under the Creative Commons Attribution License.

The mathematical expression for the upper and lower conduction subbands in the BAC approach can be expressed by the following determinant (Shan, et al., 2000):

$$\begin{vmatrix} E_N - E(k) & V_{MN} \\ V_{MN} & E_M - E(k) \end{vmatrix} = 0 \quad (1)$$

The matrix element V_{MN} is dependent on the nitrogen concentration with fraction y using following expression:

$$V_{MN} = C_{MN}\sqrt{y} \quad (2)$$

where C_{MN} is the coupling parameter that illustrates the combination between conduction bands and valance bands of extended heavy hole (HH) states, light hole (LH) states, and spin-orbit split-off (SO) states, respectively (Lindsay and O'Reilly, 1999).

$$E_{\mp}(k) = \frac{1}{2}\left(E_N + E_M(k) \mp \sqrt{\left(E_N - E_M(k)\right)^2 + 4V_{MN}^2}\right) \quad (3)$$

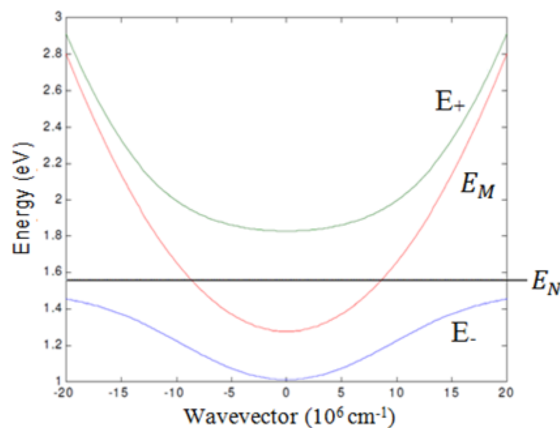

Fig. 1. Schematic of the band structure of GaInNAs, using the BAC model. The splitting of the conduction band into E- and E+ bands is clearly shown (Aissat, et al. 2007).

In this article, the cavity of VCSOA device consists of multi quantum wells (MQWs) distributed equally in three stacks forming a cavity of $3\lambda/2n_c$ long. Holes and electrons are injected through the un-doped top and bottom mirrors, respectively, pass through the QWs, recombine and generate photons. The reflectivities of the top and the bottom DBR mirrors VCSOA are designed using Fabry Perot models. The model includes optical gain and amplifier bandwidth in both reflection and transmission modes.

II. Material and Method

VCSOAs can be operated in reflection and transmission modes, depending on the reflectivity from the DBR mirrors. The reflected and transmitted light can be determined by applying the boundary conditions to Maxwell's equation of electromagnetism. The active region of GaInNAs/GaAs is enclosed between two dielectric mirrors of front and back reflectivities. Electrons and holes are injected into the active region uniformly through the surface of the confinement layers.

VCSOA designs need to fit a large number of QWs into more than two stacks to achieve a high gain that is matched to the standing wave pattern in the cavity. However, incorporating a large number of QWs makes it difficult to achieve uniform carrier distribution by using electrical injection, where the gain in QWs is no longer homogenous. The QWs should be pumped as close to full inversion as possible, in order to achieve the lowest noise figure. The standing wave effect (gain enhancement) increases with decreased number of QWs per standing wave peak. When the spacer layers are doped as in an electrically pumped device, there will be a trade-off between gain enhancement and absorption loss. If higher gain is desired, the maximum number of QWs is limited by the pumping process and it is difficult to pump uniformly using electrical injection. Accordingly, the amplification process takes place in an active region.

Gain models have been used to determine the gain spectra, which is based on the Fabry-Perot (FP) for gain calculations. The signal intensity gain of a VCSOA in reflection mode G_r and transmission mode G_t can be considered as a total of the reflection on the top DBR and the reflected part from the cavity (Adems, Collins and Henning, 1985).

$$G_r = \frac{\left(\sqrt{R_t} - \sqrt{R_b} g_s\right)^2 + 4\sqrt{R_t R_b} g_s \sin^2 \emptyset_s}{\left(1 - \sqrt{R_t R_b} g_s\right)^2 + 4\sqrt{R_t R_b} g_s \sin^2 \emptyset_s} \quad (4)$$

$$G_t = \frac{(1 - R_t)(1 - R_b) g_s}{\left(1 - \sqrt{R_t R_b} g_s\right)^2 + 4\sqrt{R_t R_b} g_s \sin^2 \emptyset_s} \quad (5)$$

Where, R_t is the reflectivity of the top DBR mirror, R_b is the reflectivity of the bottom DBR mirror, and g_s is the single pass gain. As mentioned before, DBRs can be calculated using the transfer matrix method, but can be also simulated as a fixed mirror positioned from the boundary with the incident medium and having effective reflectivity (Coldren and Corzime, 1995) of:

$$R_{DBR} = R_{t,b} = \left(\frac{1 - qp^{N-1}a}{1 + qp^{N-1}a}\right)^2 \quad (6)$$

where $q = \frac{n_{lowI}}{n_{highI}}, p = \frac{n_{low}}{n_{high}}$, and $a = \frac{n_{lowE}}{n_{highE}}$ are low and high refractive index ratios at the incident, internal and exit interfaces.

The gain is limited by either the lasing action or by the maximum material gain available. The gain of a reflection-format VCSOA and the resonance $\emptyset_s$ (Björlin, Kimura and Bowers, 2003) are given by:

$$G_R = \frac{\left(\sqrt{R_t} - \sqrt{R_b} g_s\right)^2}{\left(1 - \sqrt{R_t R_b} g_s\right)^2} \quad (7)$$

$$\emptyset_s = 2\pi n_c L_c \left(\frac{1}{\lambda} - \frac{1}{\lambda_R}\right) \quad (8)$$

Where $\emptyset_s$, n_c, L_c, are the single pass phase detuning, the refractive index of the optical cavity and the total cavity length, respectively. λ, λ_R are a signal wavelength and the resonant wavelength of the cavity.

The single pass gain in a VCSOA can be calculated from the active region of material gain g using:

$$g_s = exp[\xi g L_a - \alpha_i L_c] \quad (9)$$

where L_a, α_i, ξ are referred to as the thickness of the QWs, the average cavity loss coefficient and the gain enhancement factor, respectively. In our calculation we assume that the single pass gain g_s is varying from $(R_b)^{-0.5}$ to $\left(R_f R_b\right)^{-0.5}$, in which the laser threshold is reached when $\left(R_f R_b\right)^{-0.5} = 1$.

The optical gain depends on the QW carrier density (N), the signal wavelength (λ), the temperature (T), and the photon density (S), at room temperature and low photon densities. The QW material gain g can be approximated by (Coldren and Corzine, 1995).

$$g = g_0 ln\left[\frac{N + N_s}{N_{tr} + N_s}\right] \quad (10)$$

where g_0, N_{tr} and N_s are the gain coefficient, the carrier density concentration at transparency and the fitting parameters, respectively.

The gain bandwidth can also describe the amplifier. The gain bandwidth in reflection and transmission mode is restricted by the line width of the Fabry-Perot modes and can be obtained by (Piprek, Björlin and Bowers, 2001).

$$\Delta f_R = \frac{c}{\pi n_c L_c} \times arcsin\left\{4\sqrt{R_f R_b} G_s \left[\left(1 - \sqrt{R_f R_b} G_s\right)^{-2} - 2\left(\sqrt{R_f} - \sqrt{R_b} G_s\right)^{-2}\right]\right\}^{-1/2} \quad (11)$$

$$\Delta f_T = \frac{c}{\pi n_c L_c} \times arcsin\left\{\left(4\sqrt{R_f R_b} G_s\right)^{-1} \times \left(1 - \sqrt{R_f R_b} G_s\right)^2\right\}^{1/2} \quad (12)$$

where R_f and R_b are referred to in-front and back reflectivities in both reflection and transmission modes, respectively.

III. Results and Discussion

There is a useful simulation steps used to design the structure of VCSOA at 1.3 µm wavelength. A comprehensive model of a VCSOA includes the optical model and the optical gain. In this article, an optical design relies on the determination of the epitaxial layer contrast, layer thickness and the reflectivity dependence upon wavelength. The refractive index versus aluminum (Al) concentration for $Al_xGa_{1-x}As$ mirrors and the influence of the index contrast ratio are given in Fig. 2-a and Fig. 2-b. It is clear with high index contrast ratio, only a small number of pairs are required to achieve a given reflectivity. The peak reflectivity depends on the number of quarter wavelength layers, the refractive indices of the incident and exit media, and the high and low refractive index materials. Increasing the number of DBR layers increases the mirror reflectivity, while increasing the refractive index contrast between the materials in DBRs increases both reflectivity and the bandwidth. Thus, Bragg Reflectivities have significant consequence on the amplifier results including gain, amplifier bandwidth, figure noise and saturation output power.

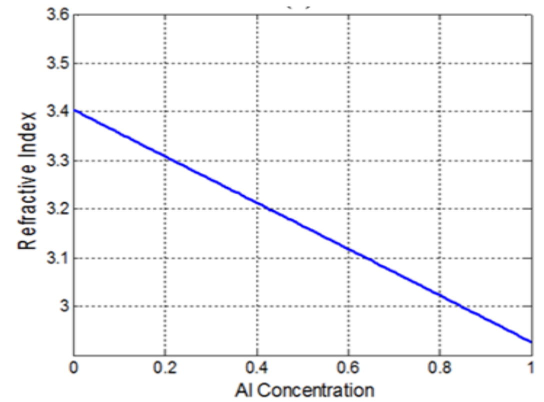

(a)

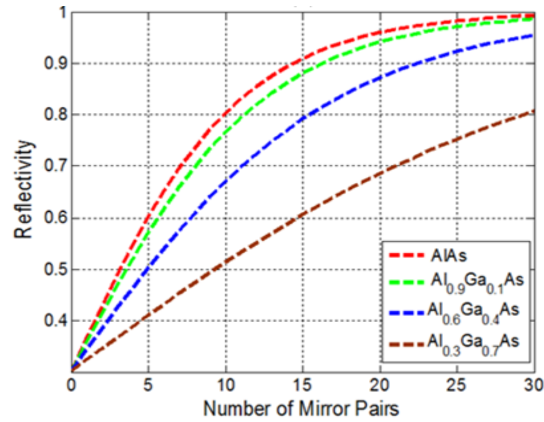

(b)

Fig. 2. Distributed Bragg Reflector illustrates: (a) the reflective index versus different Al concentration for $Al_xGa_{1-x}As$ mirrors, and (b) the influence of the refractive index contrast ratio.

Fig. 3 shows the front mirror versus bottom mirror reflectivities as a function of single pass gain G_s. The lines indicated to the lasing threshold, where the lowest excitation level is dominated by stimulated emission rather than by spontaneous emission. Below threshold, the laser's output power increases slowly with increasing excitation. A VCSOA is required to operate below threshold according to the

equation of $G_s\sqrt{R_f}\sqrt{R_b} < 1$ to avoid lasing. The small G_s requires relatively high Bragg mirror reflectivities to increase the total signal gain.

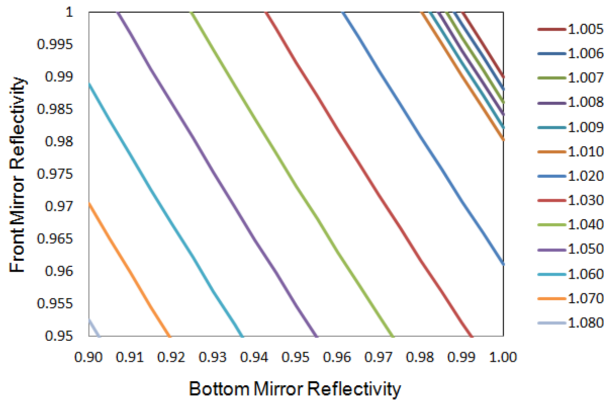

Fig. 3. The lasing threshold lines, in which the amplifier needs to operate at $G_s\sqrt{R_f}\sqrt{R_b} < 1$ to avoid lasing.

The relation between material gain and carrier density is calculated by MATLAB® program as illustrated in Fig. 4. To show general trends using an established model, material gain value can be estimated according to the parameter approximation (Lanurand, et al., 2005) using (10). The material gain has a logarithmic tendency but it is almost linear below and bove the carrier transparency of 1.18×10^{18} cm^{-3} and 6.4×10^{18} cm^{-3}, respectively.

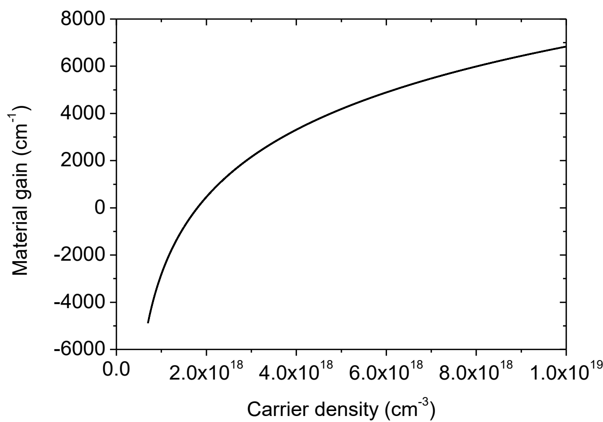

Fig. 4. Material gain versus carrier density curve for GaInNAs/GaAs QW active region.

In order to show the gain effect of the VCSOA, (4) and (5) can be used to calculate the peak gain. The peak gain of the device (or chip) depends on three parameters of the top mirrors, the bottom mirrors and the single pass gains. Fig.5 and Fig.6 presents the gain spectra in reflection and transmission modes using different single pass gains. By increasing the gain spectrum, the VCSOA bandwidth is became narrower for signal amplifying optical filter.

To illustrate the relation between VCSOA gain and its bandwidth, (4) and (5) were used to obtain the gain bandwidth using different top Bragg mirrors. The equation is mainly restricted by the line-width of the Fabry-Perot modes and it used to understand the amplifier properties of the VCSOA device in reflection mode. In high reflectivities, a net gain is demonstrated where the device start lasing, while in low reflectivities, a higher carrier density and wider gain amplifier bandwidth is obtained. However if the reflectivity is too low, there will not be enough signal pass gain. The amplifier gain bandwidth is usually measured from the optical width of the gain spectrum at the full-width half-maximum (FWHM). Amplifier bandwidth versus peak reflection gain for 24-periode bottom mirrors and various top mirrors reflectivities are shown in Fig. 7 It's clear from the figure that the amplifier bandwidth in reflection mode decreases as the peak reflection gain increases. The higher reflectivity allows for high gain and lower amplifier bandwidth. The small bandwidths are advantageous for optical filter to reduce the signal noise, while the larger bandwidths are desirable for devices used in applications with multiple channels.

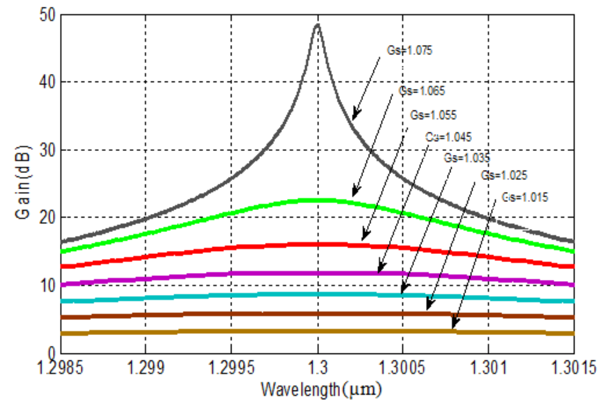

Fig. 5. Reflection VCSOA gains spectra for different Gs value, where $Rf = 0.867\%$, $Rb = 0.997\%$ and $Lc = 3\lambda/2nc$.

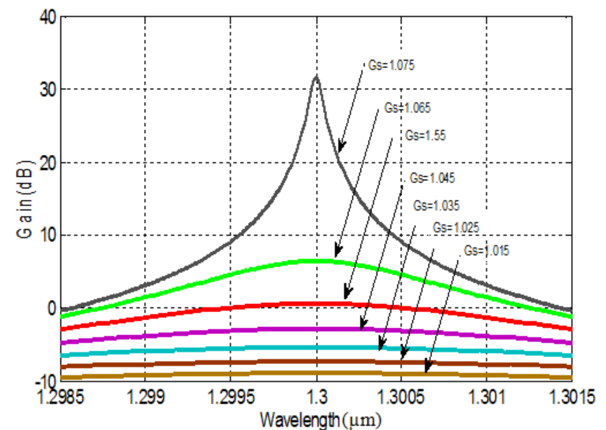

Fig. 6. Transmission VCSOA gains spectra for different Gs value, where $Rf = 0.867\%$, $Rb = 0.997\%$ and $Lc = 3\lambda/2nc$.

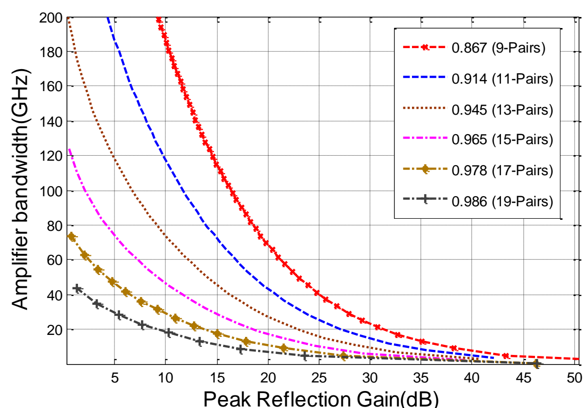

Fig. 7. Amplifier bandwidth in reflection mode versus peak reflection gain for 0.997 (24-Pairs bottom mirror) and top mirror's reflectivity for different numbers of pairs.

IV. Conclusion

In conclusions, vertical cavity semiconductor optical amplifiers VCSOAs based GaInNAs/GaAs quantum wells QWs have been designed using MATLAB® program. Device analyses are based on the theory of the Fabry-Perot semiconductor optical amplifier (SOA). VCSOAs are usually made by sandwiching a thin layer of high optical gain between two epitaxial growths of distributed Bragg mirrors (DBRs). Once the correct composition of material is selected for operating at 1.3 μm emission wavelength, the design is moved to the Bragg mirrors with different Al composition and into dilute nitride QWs in an active region. In VCSOAs, mirror with high reflectivity are necessary to reduce the resonant cavity losses and to achieve stimulated emission process. In VCSOAs, the decreased top mirror reflectivity allows for the higher pump power to achieve a higher saturation output power without losing gain.

Acknowledgment

F.A.I. Chaqmaqchee is gratefully acknowledges the financial support of the ministry of higher education and scientific research in Baghdad/Iraq during her study at University of Essex in UK.

References

Adams, M.J., Collins, J.V. and Henning, I.D., 1985. Analysis of semiconductor laser optical amplifiers. *IEE Proc. J*., 132(1), pp.58-63.

Aissat, A., Nacer, S., El-Bey, M., Guessoum, A., Ferdjani, K., Berkani, D. and Vilcot, J.P., 2007. The effect of nitrogen on the energy gap of a structure with strained quantum well containing GaInNAs/GaAs. *Iranian J. of Elect. and Comp. Eng*., 6(2), pp.169-161.

Buyanova, I.A., Chen, W.M. and Monemar, B., 2001. Electronic properties of Ga(In)NAs alloys. *MRS Internet J. Nitride Semicond. Res*., 6(2), pp.2.

Björlin, E.S., Kimura, T. and Bowers, J.E., 2003. Carrier-confined vertical cavity semiconductor optical amplifiers for higher gain and efficiency. *IEEE J. Select. Topics Quant. Elect*., 9(5), pp.1374-1385.

Coldren, L.A, Corzine, S.W. 1995. Diode lasers and photonic integrated circuits, *NY: Wiley, New York*.

Kondow, M., Uomi, K., Niwa, A., Kitatani, T., Watahiki, S. and Yazawa, Y., 1996. GaInNAs: A novel material for long-wavelength-range laser diodes with excellent high-temperature performance. *Jpn. J. Appl. Phys*., 35(1), pp.1273-1275.

Laurand, N., Calvez, S., Dawson, M.D., Bryce, A.C., Jouhti, T., Konttinen, J. and Pessa, M., 2005. Performance comparison of GaInNAs vertical cavity semiconductor optical amplifiers. *IEEE J. Quant. Elect.*, 41(5), pp.642-649.

Lindsay, A. and O'Reilly, E.P., 1999. Theory of enhanced bandgap non parabolicity in GaN_x As_{1-x} and related alloys. *Solid State Commun*ication. 112(8), pp.443-447.

Piprek, J., Björlin, E.S. and Bowers, J.E., 2001. Design and analysis of vertical-cavity semiconductor optical amplifiers. *IEEE J. Quant. Elect.*, 37(1), pp.127-134.

Piprek, J., Bjorlin, E.S. and Bowers, J.E., 2001. Optical gain-bandwidth product of vertical cavity laser amplifiers. *Elect. Letts.*, 37(5), pp.298-299.

Shan, W., Walukiewiez, W., Ager, J.W., Haller, E.E., Geisz, J.F., Friedman, D.J., Olson J.M. and Kurtz, S.R., 1999. Band anticrossing in GaInNAs alloys. *Phys. Rev. Lett.*, 82(6), pp.1221.

Skierbiszewski, C., Perlin, P., Wišniewski, P., Knap, W., Suski, T., Walukiewicz, W., Shan, W., Yu, K.M., Ager, J.W., Haller, E.E., Geisz, J.F. and Olson, J.M., 2000. Large, nitrogen-induced increase of the electron effective mass in $In_yGa_{1-y}N_xAs_{1-x}$. *Appl. Phys. Lett.* 76(17), pp.2409-2411.

Sun, Y., Balkan, N., Erol, A. and Arikan, M.C., 2009. Electronic transport in n- and p-type modulation-doped GaInNAs/GaAs quantum wells. *Microelect. J.*, 40(30), pp.403-405.